applied optics

High efficient generation of over 1 Watt 509 nm laser beam by a ring cavity frequency doubler with periodically poled $KTiOPO_4$

Gang Li,[1,2,*] Shaokang Li,[1] Xingchang Wang,[1] Pengfei Zhang,[1,2] and Tiancai Zhang[1,2]

[1]State Key Laboratory of Quantum Optics and Quantum Optics Devices, and Institute of Opto-Electronics, Shanxi University, Taiyuan 030006, China
[2]Collaborative Innovation Center of Extreme Optics, Shanxi University, Taiyuan 030006, China
*Corresponding author: gangli@sxu.edu.cn

Received 9 September 2016; revised 18 November 2016; accepted 29 November 2016; posted 5 December 2016 (Doc. ID 273860); published 22 December 2016

We report high efficient generation of a 509 nm laser beam by a ring cavity frequency doubler with a periodically poled $KTiOPO_4$ (PPKTP) crystal. A maximum power of 1.13 W at 509 nm cw light is obtained with mode-matched power of 1.58 W, corresponding to a conversion efficiency of 71.5%. By using the Hänsch–Couillaud locking technique, the doubler is locked with high stability, and power fluctuation smaller than ±0.5% within 1 h is achieved at the maximum output. To the best of our knowledge, this is the highest second-harmonic power produced by a cavity-enhanced PPKTP frequency doubler below 532 nm.

OCIS codes: (190.2620) Harmonic generation and mixing; (140.3515) Lasers, frequency doubled.

https://doi.org/10.1364/AO.56.000055

1. INTRODUCTION

Second-harmonic generation (SHG) is now a standard technique to produce laser beams with shorter wavelength, especially in the green and blue region, where high power and high stability direct laser sources are hard to obtain. In many quantum metrology, quantum information, and quantum state manipulation experiments [1–9], stable, high-power cw laser beams with shorter wavelength are always needed, and frequency doubling of longer wavelength lasers by nonlinear crystal is commonly adopted. Among many nonlinear materials used for SHG, periodically poled $KTiOPO_4$ (PPKTP) is one of the most attractive crystals for generation of low and medium power of second-harmonic (SH) light waves due to its relatively high nonlinear coefficients, low photorefractivity, low quasi-phase-matching temperature, and low cost [10,11]. At the same time, because of the lack of high-power fundamental laser sources in these regions, the Ti:sapphire laser or amplified diode laser light is usually frequency doubled by cavity-enhanced SHG configuration for its higher conversion efficiency than single-pass SHG configuration. By using a cavity-enhanced PPKTP frequency doubler, cw SH waves of various wavelengths from UV to near-infrared have been produced [10–22]. However, due to thermal issues accompanying the SHG process, the produced SH power could not reach its theoretical maximum in these experiments. In order to get a higher SH power, the problems of the thermal effect need to be addressed.

KTP crystal shows bigger absorption at shorter wavelengths in the visible and near-infrared region, so the absorption of the SH wave is usually much bigger than that of a fundamental wave [23]. These absorptions can not only directly decrease the SHG efficiency, but also induce thermal effects, such as thermal lensing and thermal dephasing, which affect the conversion efficiency in different ways. The thermal lensing effect [10,24] will deform the spatial mode of enhancing cavity and change the mode-matching condition of the fundamental beam to the enhancing cavity. Thus, the overall SHG conversion efficiency will be decreased if the thermal lens deteriorates the mode-matching condition. The reason for thermal dephasing in PPKTP is complicated [25], and thermal dephasing appears when the input power exceeds some threshold and exists in both single-pass [26] and enhancing-cavity configurations [27]. In the cavity-enhanced SHG configuration, thermal lensing not only affects the mode coupling of the fundamental wave to the enhancing cavity but also induces bistability at high powers, which makes the cavity hard to be actively locked to its fringe maximum. In 2005, Targat *et al.* proposed that by choosing longer PPKTP crystals and looser focusing, the thermal lensing effect could be relieved without lowering the conversion efficiency. They also demonstrated generation of a 234 mW light beam at 461 nm with 75% conversion efficiency [10]. However, even by adapting a similar method, stable watt-level power SHG could only be obtained in the

low-absorption region for a PPKTP-based cavity-enhancing frequency doubler at longer wavelengths. In 2011, Ast *et al.* realized 1.05 W 775 nm generation with conversion efficiency of about 95% by using a PPKTP-based semimonolithic standing-wave cavity [21]. In their experiment, the PPKTP absorptions of fundamental 1550 nm and SH 775 nm waves are extremely low, and the induced thermal effects are not obvious. In 2013, by using a 10 mm × 1 mm × 1 mm PPKTP crystal, Zhang *et al.* demonstrated 1.2 W at 532 nm with 72% conversion efficiency in a ring-enhancing cavity [11]. To the best of our knowledge, there is no report on generation of watt-level cw light wave below 532 nm by a cavity-enhanced PPKTP frequency doubler with high stability.

In this paper, we report over 1 W laser-wave generation at 509 nm by using a 10 mm × 2 mm × 1 mm PPKTP crystal in a ring cavity with a robust design, and by adapting a loose focusing condition [22]. A maximum power of 1.13 W cw light is obtained with mode-matched fundamental power of 1.58 W, corresponding to a conversion efficiency of 71.5%. In our experiment, the thermal-induced bistability is relieved so that the doubler can be actively locked by using the Hänsch–Couillaud locking technique [28]. The doubler shows high stability at all power levels; the fluctuation is smaller than ±0.5% within 1 h at the maximum output power of 1.13 W. Watt-level beams at 509 nm not only have potential application in pumping Ti:sapphire laser to get good beam quality and power stability [29], but also can be used to manipulate the Rydberg state of cesium atoms through the two-photon process [30].

2. EXPERIMENT AND RESULTS

In our frequency doubler, the enhancing cavity is a ring cavity with a bow-tie configuration (Fig. 1), in which M1 and M2 are plane mirrors and M3 and M4 are concave mirrors with same curvature radius, $r = 75$ mm. To build a stable and compact cavity, all the 12.7 mm size mirrors are mounted on a top-adjusted mirror mount (9814-6-K, NewPort) [31]. The mirror

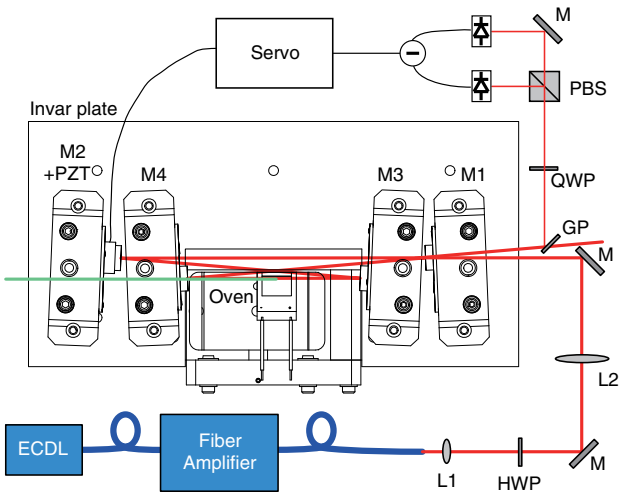

Fig. 1. Schematic of the SHG experiment setup. M1, M2, M3, and M4 are cavity mirrors mounted on a top-adjusted mirror mount. ECDL, external cavity diode laser; HWP, half-wave plate; QWP, quarter-wave plate; M, high-reflected mirrors; GP, glass plate; PBS, polarization beam splitter.

mounts have a mounting size of 25.4 mm, so all the mirrors are mounted at one side of the mounting aperture through an adapter, and another side is clear to pass light beams. This configuration can compress the folding angle of the cavity to 4.8°. M2 is attached with a piezoactuator (PZT) to actively lock the cavity. The mirror mounts are firmly mounted on a 10 mm-thick Invar plate and enclosed with a well-sealed aluminum box to improve stability. The total cavity length is about 488 mm, corresponding to a free spectral range of 606 MHz, and the distance between M3 and M4 is about 88 mm. A 10 mm × 2 mm × 1 mm PPKTP crystal (Raicol Crystals, Israel) with poling period of 7.75 μm is housed in a homemade copper oven and placed between M3 and M4 with equal distance to them. The temperature of the oven is controlled by a Peltier part with temperature-controlling accuracy better than 0.01°C. The waist size of the primary cavity mode is $w_0 = 37$ μm and lies in the middle of the crystal. This gives a confocal parameter of $b = kw_0^2 = 21$ mm and focusing condition of $l/b = 0.48$, which is about 6 times smaller than the optimum value 2.88 proposed by Boyd and Kleinman [32] in order to improve the thermal issues [10,22].

M1 is the input-coupling mirror with transmission $T_1 = 8.7 \pm 0.5\%$ at 1018 nm. M2 and M3 are high-reflective coated with reflectivity $R_{2,3} > 99.9\%$. M4 is a dichroic mirror with high reflectivity, $R_4^{1018} = 99.3 \pm 0.1\%$ at 1018 nm, and high transmission $T_4^{509} = 95.6 \pm 0.1\%$ at 509 nm. Both end facets of the crystal are antireflection-coated with claimed reflectivity $R < 0.1\%$ at both 1018 nm and 509 nm. However, when the PPKTP is working far from phase-matching temperature, the measured cavity finesse is 57 ± 1, which gives a total intracavity loss of $10.3 \pm 0.2\%$. This means that the PPKTP crystal introduces extra loss of about 0.6%–0.8% for the 1018 nm fundamental wave in our experiment.

Our fundamental 1018 nm wave comes from a fiber amplifier (MFAP-1018-B-MP, Connet Fiber Optics) with maximum output power of 2.2 W. The seed laser is a homemade external cavity diode laser composed by an AR (anti-reflection)-coated laser diode (EYP-RWE-1060-10020-0750-SOT01-0000, Eagleyard) and a 1200 line/mm grating in Littrow configuration. In this configuration, the first order of diffraction from the grating is feedback into the diode. Due to the optical dispersion of the grating, only power in certain small parts of the spectrum range is fed back into the diode and being amplified. The output of the fiber amplifier is coupled out by a polarization-maintaining fiber (PM980-XP, Nufern). The spatial mode of output beam is transformed by a $f = 8$ mm aspheric lens (L1) and a $f = 250$ mm lens (L2) and spatially overlaps with the cavity TEM_{00} mode through its secondary mode with waist $w_0' = 230$ μm.

To characterize the SHG process in the enhanced cavity, single-pass SHG performance of the PPKTP crystal sample is tested. In this measurement, M1 is replaced by a same thick antireflection coated glass plate (GP); thus, the same fundamental beam waist and position are achieved in the PPKTP crystal as that of the closed cavity. The dependence of single-pass SH power on crystal temperature is measured with a fundamental wave power of 480 mW. The inset of Fig. 2 gives the normalized SH power versus temperature, and the

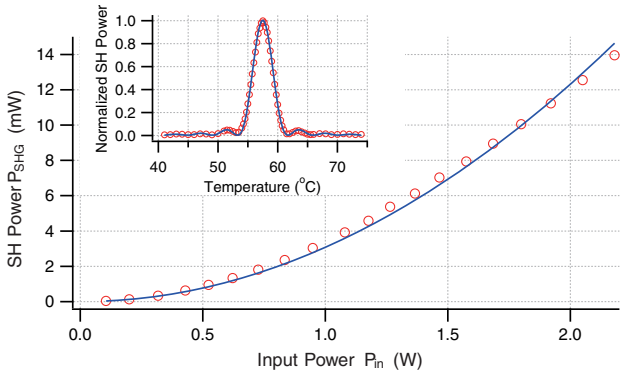

Fig. 2. Single-pass SH power P_{SHG} versus input fundamental wave power P_{in}, where the solid blue curve is the quadratic fitting. The fitting gives $E_{NL} = 0.31 \pm 0.05\%\ W^{-1}$. Inset is single-passed SH power versus crystal temperature, where the solid curve is a sinc^2 function fit. The optimum phase-matching temperature of 57.5°C and FWHM of 3.7°C are extracted from the fitting.

solid curve is the fitting. We can see the optimum phase-matching temperature is 57.5°C, and temperature tuning bandwidth FWHM = 3.7°C. Next, the PPKTP temperature is tuned to 57.5°C, and measurements of single-passed SH power P_{SHG} on different input fundamental power P_{in} are performed. Figure 2 gives the results, in which the solid blue curve is the quadratic fitting $P_{SHG} = E_{NL}P_{in}^2$ with only one fitting parameter, E_{NL}. We then get the single-pass conversion efficiency $E_{NL} = 0.31 \pm 0.05\%\ W^{-1}$ for our PPKTP sample in our low-focusing condition.

The input coupler M1 is then retrieved back to close the cavity, and the performance of the cavity-enhanced SHG is investigated. Assume the TEM_{00} mode-matching factor is η; for an input fundamental wave with power P_{in}, the resonant intracavity power P_c can be expressed by [10]

$$P_c = \frac{T_1 P_{in}\eta}{(1 - \sqrt{(1 - T_1)(1 - l)}(1 - (E_{NL} + E_{abs})P_c))^2}, \quad (1)$$

where E_{abs} is the efficiency of the SH absorption, l is the extra fundamental round-trip losses of cavity excluding T_1, and losses due to the SHG process are $(E_{NL} + E_{abs})P_c$. The reflected beam from a TEM_{00} mode-resonant cavity contains two parts: (1) power that is not coupled to the cavity TEM_{00} mode, for which the power reflection is described by $(1 - \eta)$; (2) power P_{00} in TEM_{00} mode is reflected due to imperfect impedance matching, and the power reflection is expressed by [33]

$$R_{00} = \left(\frac{\sqrt{(1 - l)(1 - (E_{NL} + E_{abs})P_c)} - \sqrt{1 - T_1}}{1 - \sqrt{(1 - T_1)(1 - l)}(1 - (E_{NL} + E_{abs})P_c)}\right)^2. \quad (2)$$

So, the total power reflection of the cavity is then

$$R_c = (1 - \eta) + \eta R_{00}. \quad (3)$$

From these equations, we can see that in order to couple more fundamental wave power into the frequency doubler, both the TEM_{00} mode-matching factor and impedance-matching factor should be increased. The TEM_{00} mode-matching factor in the cavity-enhanced SHG process is not only determined by the cavity structure but also influenced by the thermal lensing effect. The dominant origin of thermal lensing effect is green-light-induced IR absorption (GLIIRA), which is associated with the SHG process. The thermal lensing will be serious for high intracavity power. Even though a high TEM_{00} mode-matching factor is achieved in the low-power level, it will decrease with the rising of intracavity power. The perfect impedance happens when $R_{00} = 0$, which gives an optimum value $T_1 = l + (E_{NL} + E_{abs})P_c$. Given a perfect TEM_{00} mode-matching factor of $\eta = 1$ and nonabsorption of PPKTP, combined with Eq. (1), the optimum value of T_1 for our cavity is found to be 9.3% for 2.0 W input power. In our experiment, $T_1 = 8.7 \pm 0.5\%$, which is very close to the optimum value, and the theory gives cavity reflection below 1% for input fundamental power $P_{in} > 1.2$ W under perfect mode-matching conditions.

The reflection of the cavity under different input fundamental power P_{in} is displayed in Fig. 3 when the cavity is locked and SHG is optimized to its maximum. From this figure, we can see that the reflection goes down rapidly with the rise of input power P_{in} at low-power levels and goes up slowly at high-input power levels. As we have discussed, two effects govern the reflection at different power levels. At low-power levels, the thermal lensing effect is small, and the reflection is mainly due to the imperfect impedance matching. The impedance matching is continually improved with an increase of input power, so the reflection drops. We found, in theory, that the cavity reflection will drop below 1% for a perfect mode-matched input fundamental wave with power $P_{in} > 1.2$ W. However, due to the more severe thermal lensing effect at a higher power level, the mode matching cannot reach this theoretical value, and we could only get a reflection of 22% here. When the input power is increased above 1.2 W, the thermal lensing effect becomes dominant, which deteriorates the TEM_{00} mode-matching condition, and thus the reflection increases again. The TEM_{00} mode-matching factor could be extracted by using Eqs. (1)–(3). The extracted mode-matching factor and intracavity power versus input power are shown in the inset of Fig. 3. We can see that the mode-matching factor improved at the low-power level and deteriorated at the high-power level. The maximum mode-matching factor is about 82.4% at

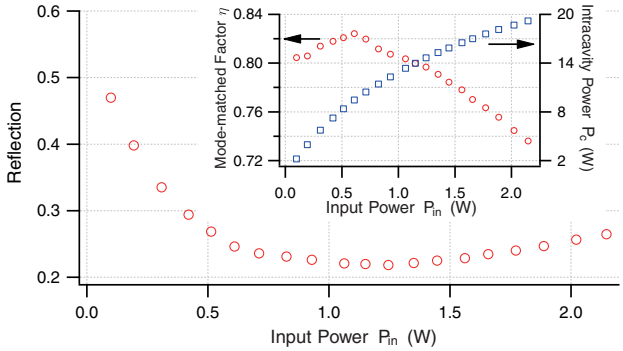

Fig. 3. Reflection of the SHG cavity at sample points of the input power when the cavity is locked and SHG is optimized to maximum. Inset is the plot of the calculated mode-matching factor η and intracavity power P_c by using Eqs. (1)–(3).

0.62 W, and the lowest mode-matching factor is about 73% at 2.2 W. Different from the mode-matching factor η, the intracavity power P_c keeps increasing with the rise of input power.

By using the extracted mode-matching factor η, the mode-matched fundamental power P_{00} can be calculated. The dependence of generated SH power P_{SHG} and conversion efficiency ϵ on mode-matched fundamental power P_{00} is shown in Fig. 4(a). We can see that a maximum SHG power of 1.13 W at 509 nm with mode-matched fundamental power of 1.58 W can be obtained, and the corresponding SHG conversion efficiency is 71.6%. The dashed lines are theoretical predictions by $E_{NL}P_c^2$, with intracavity power P_c calculated by assuming $E_{abs} = 0$. However, there exists an obvious disparity between theory and experiment at high pump power. When $E_{abs} = 0.04\%$ is taken into account, the theoretical curves, shown as solid lines in Fig. 4(a), are in good accordance with the experiment. The change of SH power P_{SHG} with intracavity power P_c is displayed in Fig. 4(b). We also show the theoretical expectation by $P_{SHG} = E_{NL}P_c^2$, as well as the single-pass SHG data in the same figure for comparison. We can see that the experimental results are in good agreement with the theory, and no thermal dephasing occurs in our experiment.

We did not observe serious bistability induced by heating when the cavity is scanned at all power levels in our experiment. The inset of Fig. 5 shows the reflection of SHG cavity with 2.2 W pump power and 1.13 W output of 509 nm SH wave. The bistability observed does not deteriorate the robust

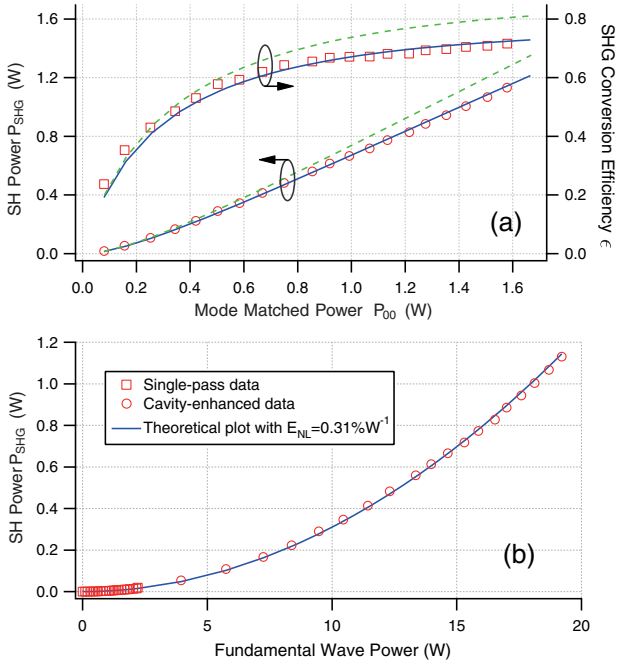

Fig. 4. (a) SH power P_{SHG} (red circles; refer to the left axis) and the corresponding SHG efficiency ε (red squares; refer to the right axis) for different sample points of mode-matched power P_{00}. Green dashed curves and blue solid curves are the corresponding theoretical predictions with $E_{abs} = 0$ and $E_{abs} = 0.04\%$. (b) The change of SH power P_{SHG} with intracavity power P_c (red circles). Red squares are the single-pass SHG data shown in Fig. 2. Blue solid curve is the theoretical expectation by $P_{SHG} = E_{NL}P_c^2$.

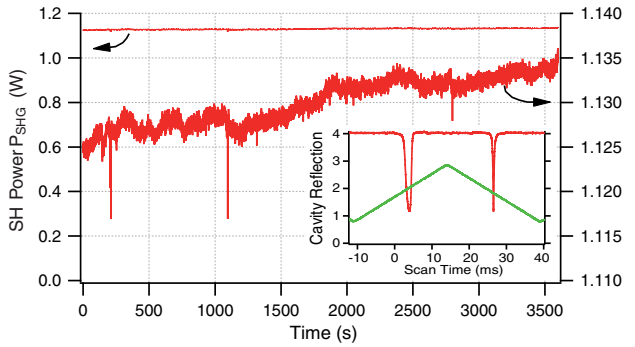

Fig. 5. Record of SH power P_{SHG} fluctuation in 1 h at the maximum value of 1.13 W. The small spikes are due to some sudden mechanical shock, and the overall fluctuation is smaller than $\pm 0.5\%$. The top line gives the power fluctuation in full observation range (left axis) and the bottom line is the enlarged fluctuation to show more details (right axis). Inset figure is reflection of the SHG cavity with $P_{in} = 2.2$ W pump power and $P_{SHG} = 1.13$ W output of 509 nm SH wave. The upper red curve is the cavity reflection and the bottom green triangular wave is the ramp signal applied to the cavity PZT.

standard Hänsch–Couillaud technique [28], which is adopted to actively lock the cavity. As shown in Fig. 1, part of the reflected beam from the cavity is coupled out by a GP and sent to a polarization analyzer composed by a quarter-wave plate (QWP) and polarization beam splitter (PBS). The output of the polarization analyzer is then detected by homodyne detector to produce the error signal, which is finally fed back to the PZT attached with M3 through an electronic servo system to actively lock the cavity.

In order to maximize the output SH power P_{SHG} at a given input power level, the phase-matching temperature needs to be optimized to compensate the heating of PPKTP by fundamental wave and SH wave absorption. At a pump level of 2.2 W, the temperature of the PPKTP needs to be tuned to 54.4°C, and 1.13 W of SH power can be generated with mode-matched power of 1.58 W. Benefiting from the robust design of the cavity and the wide capture range of the error signal produced by the Hänsch–Couillaud locking technique, the SH power shows high stability when the cavity is locked. Fig. 5 is a record of the fluctuation of the SH power at a maximum level of 1.13 W for an hour, where the small spikes are due to some sudden mechanical shock. We can see that the overall fluctuation is less than $\pm 0.5\%$, including a slow drift of power. There are two possible reasons for this slow drift: (1) slow variation of the PPKTP temperature at high pumping power level. The heating of the PPKTP crystal is more severe at high pumping power levels; thus it is more difficult to control the phase-matching temperature. Slow drift of the actual crystal temperature could occur. (2) The slow drift of the baseline of the locking signal. The error signal for locking is produced by homodyne detection of output of the polarization analyzer; any tiny drift of the beam power or electrical bias in the detector could cause the baseline of the error signal to change and finally make the output power drift. To get more stable output power, further optimizing of these two parts needs to be done.

3. DISCUSSION

As we discussed before, the absorption of KTP crystal cannot be omitted at shorter wavelengths. So, in order to get higher output SHG power on even shorter wavelengths, the dependence of conversion efficiency on E_{abs} need to be investigated. In a situation with perfect mode matching $\eta = 1$ and impedance-matching condition $T_1 = l + (E_{NL} + E_{abs})P_c$, and a lossless cavity $l = 0$, from Eqs. (1) and (2) we get the mode-matched SHG conversion efficiency:

$$\varepsilon = \frac{P_{SHG}}{P_{00}} = \frac{1}{1 + \frac{E_{abs}}{E_{NL}}}, \tag{4}$$

where the SHG power $P_{SHG} = E_{NL}P_c^2$. Thus, we could see that unitary conversion efficiency can be achieved when the absorption of SH wave can be neglected; this is close to the experiment in Ref. [21], where both the absorptions of the fundamental 1550 nm and SH wave 775 nm can be omitted, and the 95% SHG conversion efficiency is mainly due to imperfect mode matching and impedance matching. When the SHG wavelength moves to the shorter wavelength band, the absorption becomes bigger. According to Ref. [23], the absorption on 532 nm is much bigger than that on 775 nm; thus, the SHG conversion efficiency drops accordingly in Ref. [11], even though they did not perform more investigations on the absorption loss. Here, in our experiment, the absorption loss on 509 nm is about 1.5 times bigger than that on 532 nm, according to Ref. [23]. Our PPKTP sample has an estimated absorption efficiency $E_{abs} = 0.04\%$, and we only get a conversion efficiency of $\eta = 71.5\%$. In order to get a higher conversion efficiency, the thermal lensing effect due to the absorption needs to be addressed at high power levels to get higher mode-matching conditions. By using our current setup, the maximum conversion efficiency of 75% can be achieved if perfect mode matching and perfect impedance matching with $T_1 = 9.5\%$ at $P_{in} = 2.2$ W are achieved, and the corresponding maximum SH power is expected to be $P_{SHG} = 1.65$ W. Of course, the single-pass conversion efficiency and absorption for PPKTP crystal are different from piece to piece, so by using better PPKTP crystals, the output power could be improved further in our experiment. If a SHG process at even shorter wavelength is considered, the increase of absorption continually lowers the conversion efficiency, according to Eq. (4). The actual conversion efficiency and maximum output are determined not only on single-pass conversion efficiency E_{NL} and absorption efficiency E_{abs} associated with the crystal one used, but also on the cavity loss l, mode-matching, and impedance-matching conditions.

4. CONCLUSION

To summarize our paper, we report high efficient generation of a 509 nm laser beam by using resonant cavity-enhanced SHG with a PPKTP crystal. By adopting a loose cavity mode waist size $w_0 = 37$ μm inside the PPKTP crystal, we got a focusing condition of $l/b = 0.48$, which is about 6 times smaller than the optimum value, 2.88. The thermal effects induced by the GLIIRA are thus dramatically depressed, and the enhanced cavity can be actively locked by the Hänsch–Couillaud locking technique. A maximum power of 1.13 W of cw laser beam at 509 nm is obtained with mode-matched power of 1.58 W, corresponding to a conversion efficiency of 71.5%. The whole system shows high stability, with fluctuation less than ±0.5% within 1 h. It is possible to get even higher SH output power and conversion efficiency by optimizing the TEM_{00} mode-matching condition at high fundamental power levels and eliminating extra cavity losses. This high-quality cw Watt-level laser beam at 509 nm can be used either in high-performance Ti:sapphire lasers as the pump, or in the field of atomic control, such as the Rydberg state manipulation of cesium atoms.

Funding. National Natural Science Foundation of China (NSFC) (11634008, 11674203, 61227902, 61275210, 91336107).

REFERENCES

1. E. S. Polzik, J. Carri, and H. J. Kimble, "Spectroscopy with squeezed light," Phys. Rev. Lett. **68**, 3020–3023 (1992).
2. L. Hesselink, S. S. Orlov, A. Liu, A. Akella, D. Lande, and R. R. Neurgaonkar, "Photorefractive materials for nonvolatile volume holographic data storage," Science **282**, 1089–1094 (1998).
3. H. Ditlbacher, J. R. Krenn, B. Lamprecht, A. Leitner, and F. R. Aussenegg, "Spectrally coded optical data storage by metal nanoparticles," Opt. Lett. **25**, 563–565 (2000).
4. S. Suzuki, H. Yonezawa, F. Kannari, M. Sasaki, and A. Furusawa, "7 dB quadrature squeezing at 860 nm with periodically poled $KTiOPO_4$," Appl. Phys. Lett. **89**, 061116 (2006).
5. F.-Y. Wang, B.-S. Shi, Q.-F. Chen, C. Zhai, and G.-C. Guo, "Efficient cw violet-light generation in a ring cavity with a periodically poled KTP," Opt. Commun. **281**, 4114–4117 (2008).
6. J. S. Neergaard-Nielsen, B. M. Nielsen, C. Hettich, K. Mølmer, and E. S. Polzik, "Generation of a superposition of odd photon number states for quantum information networks," Phys. Rev. Lett. **97**, 083604 (2006).
7. Z. Y. Ou and Y. J. Lu, "Cavity enhanced spontaneous parametric down-conversion for the prolongation of correlation time between conjugate photons," Phys. Rev. Lett. **83**, 2556–2559 (1999).
8. T. C. Zhang, K. W. Goh, C. W. Chou, P. Lodahl, and H. J. Kimble, "Quantum teleportation of light beams," Phys. Rev. A **67**, 033802 (2003).
9. H. Y. Hao, L. Tian, H. X. Yuan, L. I. Shu-Jing, and H. Wang, "The experimental investigation of 795 nm correlation photons caused by spontaneous parametric down-conversion," Acta Sin. Quantum Opt. **20**, 177–182 (2014).
10. R. L. Targat, J.-J. Zondy, and P. Lemonde, "75%-efficiency blue generation from an intracavity PPKTP frequency doubler," Opt. Commun. **247**, 471–481 (2005).
11. Y. Zhang, N. Hayashi, H. Matsumori, R. Mitazaki, Y. Xue, Y. Okada-Shudo, M. Watanabe, and K. Kasai, "Generation of 1.2 W green light using a resonant cavity-enhanced second-harmonic process with a periodically poled $KTiOPO_4$," Opt. Commun. **294**, 271–275 (2013).
12. F. Torabi-Goudarzi and E. Riis, "Efficient cw high-power frequency doubling in periodically poled KTP," Opt. Commun. **227**, 389–403 (2003).
13. F. Villa, A. Chiummo, E. Giacobino, and A. Bramati, "High-efficiency blue-light generation with a ring cavity with periodically poled KTP," J. Opt. Soc. Am. B **24**, 576–580 (2007).
14. J. H. Lundeman, O. B. Jensen, P. E. Andersen, S. Andersson-Engels, B. Sumpf, G. Erbert, and P. M. Petersen, "High power 404 nm source based on second harmonic generation in PPKTP of a tapered external feedback diode laser," Opt. Express **16**, 2486–2493 (2008).
15. X. Deng, J. Zhang, Y. Zhang, G. Li, and T. Zhang, "Generation of blue light at 426 nm by frequency doubling with a monolithic periodically poled $KTiOPO_4$," Opt. Express **21**, 25907–25911 (2013).
16. Y. Han, X. Wen, J. Bai, B. Yang, Y. Wang, J. He, and J. Wang, "Generation of 130 mw of 397.5 nm tunable laser via ring-cavity-enhanced frequency doubling," J. Opt. Soc. Am. B **31**, 1942–1947 (2014).
17. X. Wen, Y. Han, J. Bai, J. He, Y. Wang, B. Yang, and J. Wang, "Cavity-enhanced frequency doubling from 795 nm to 397.5 nm ultra-violet

coherent radiation with PPKTP crystals in the low pump power regime," Opt. Express **22**, 32293–32300 (2014).
18. K. Danekar, A. Khademian, and D. Shiner, "Blue laser via IR resonant doubling with 71% fiber to fiber efficiency," Opt. Lett. **36**, 2940–2942 (2011).
19. X. Song, Z. Li, P. Zhang, G. Li, Y. Zhang, J. Wang, and T. Zhang, "Frequency doubling with periodically poled $KTiOPO_4$ at the fundamental wave of cesium d2 transition," Chin. Opt. Lett. **5**, 596–598 (2007).
20. Y. Zhao, B.-K. Lin, Y. Li, H.-X. Zhang, J.-P. Cao, Z.-J. Fang, T.-C. Li, and E.-J. Zang, "High conversion efficiency and power stability of 532 nm generation from an external frequency doubling cavity," Chin. Phys. Lett. **29**, 094210 (2012).
21. S. Ast, R. M. Nia, A. Schönbeck, N. Lastzka, J. Steinlechner, T. Eberle, M. Mehmet, S. Steinlechner, and R. Schnabel, "High-efficiency frequency doubling of continuous-wave laser light," Opt. Lett. **36**, 3467–3469 (2011).
22. J. Tian, C. Yang, J. Xue, Y. Zhang, G. Li, and T. Zhang, "High-efficiency blue light generation at 426 nm in low pump regime," J. Opt. **18**, 055506 (2016).
23. G. Hansson, H. Karlsson, S. Wang, and F. Laurell, "Transmission measurements in KTP and isomorphic compounds," Appl. Opt. **39**, 5058–5069 (2000).
24. A. Douillet, J.-J. Zondy, A. Yelisseyev, S. Lobanov, and L. Isaenko, "Stability and frequency tuning of thermally loaded continuous-wave $AgGaS_2$ optical parametric oscillators," J. Opt. Soc. Am. B **16**, 1481–1498 (1999).
25. N. E. Yu, C. Jung, D. K. Ko, J. Lee, O. A. Louchev, S. Kurimura, and K. Kitamura, "Thermal dephasing of quasi-phase-matched second-harmonic generation in periodically poled stoichiometric $LiTaO_3$ at high input power," J. Korean Phys. Soc. **49**, 528–532 (2006).
26. S. C. Kumar, G. K. Samanta, and M. Ebrahim-Zadeh, "High-power, single-frequency, continuous-wave second-harmonic-generation of ytterbium fiber laser in PPKTP and Mgo:sPPLT," Opt. Express **17**, 13711–13726 (2009).
27. J. H. Lundeman, O. B. Jensen, P. E. Andersen, and P. M. Petersen, "Threshold for strong thermal dephasing in periodically poled KTP in external cavity frequency doubling," Appl. Phys. B **96**, 827–831 (2009).
28. T. Hänsch and B. Couillaud, "Laser frequency stabilization by polarization spectroscopy of a reflecting reference cavity," Opt. Commun. **35**, 441–444 (1980).
29. M. Tawfieq, O. B. Jensen, A. K. Hansen, B. Sumpf, K. Paschke, and P. E. Andersen, "Efficient generation of 509 nm light by sum-frequency mixing between two tapered diode lasers," Opt. Commun. **339**, 137–140 (2015).
30. J. Zhao, X. Zhu, L. Zhang, Z. Feng, C. Li, and S. Jia, "High sensitivity spectroscopy of cesium Rydberg atoms using electromagnetically induced transparency," Opt. Express **17**, 15821–15826 (2009).
31. M. Pizzocaro, D. Calonico, P. C. Pastor, J. Catani, G. A. Costanzo, F. Levi, and L. Lorini, "Efficient frequency doubling at 399 nm," Appl. Opt. **53**, 3388–3392 (2014).
32. G. D. Boyd and D. A. Kleinman, "Parametric interaction of focused Gaussian light beams," J. Appl. Phys. **39**, 3597–3639 (1968).
33. H.-A. Bachor and T. C. Ralph, *A Guide to Experiments in Quantum Optics*, 2nd ed. (Wiley, 2004).